

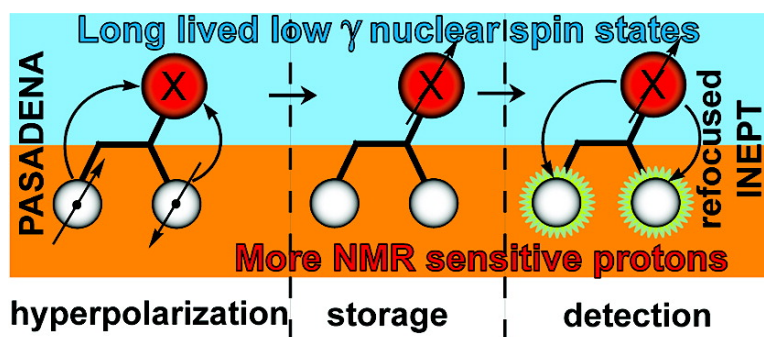
Communication

## Hyperpolarized H NMR Employing Low # Nucleus for Spin Polarization Storage

Eduard Y. Chekmenev, Valerie A. Norton, Daniel P. Weitekamp, and Pratip Bhattacharya

*J. Am. Chem. Soc.*, **2009**, 131 (9), 3164-3165 • DOI: 10.1021/ja809634u • Publication Date (Web): 16 February 2009

Downloaded from <http://pubs.acs.org> on April 27, 2009



### More About This Article

Additional resources and features associated with this article are available within the HTML version:

- Supporting Information
- Access to high resolution figures
- Links to articles and content related to this article
- Copyright permission to reproduce figures and/or text from this article

[View the Full Text HTML](#)



**ACS Publications**  
High quality. High impact.

Hyperpolarized  $^1\text{H}$  NMR Employing Low  $\gamma$  Nucleus for Spin Polarization StorageEduard Y. Chekmenev,<sup>†‡</sup> Valerie A. Norton,<sup>‡</sup> Daniel P. Weitekamp,<sup>‡</sup> and Pratip Bhattacharya<sup>\*,†</sup>

Enhanced Magnetic Resonance Laboratory, Huntington Medical Research Institutes, Pasadena, California 91105, and A. A. Noyes Laboratory of Chemical Physics, California Institute of Technology, Pasadena, California 91125

Received December 9, 2008; E-mail: pratip@hmri.org

The PASADENA (parahydrogen and synthesis allow dramatically enhanced nuclear alignment)<sup>1,2</sup> and DNP (Dynamic Nuclear Polarization)<sup>3</sup> methods efficiently hyperpolarize biologically relevant nuclei such as  $^1\text{H}$ ,  $^{31}\text{P}$ ,  $^{13}\text{C}$ ,  $^{15}\text{N}$  achieving signal enhancement by a factor of  $\sim 100\,000$  on currently utilized MRI scanners. Recently, many groups have demonstrated the utility of hyperpolarized MR in biological systems using hyperpolarized  $^{13}\text{C}$  biomarkers with a relatively long spin lattice relaxation time  $T_1$  on the order of tens of seconds.<sup>4–7</sup> Moreover, hyperpolarized  $^{15}\text{N}$  for biomedical MR has been proposed due to even longer spin lattice relaxation times.<sup>8</sup> An additional increase of up to tens of minutes in the lifetime of hyperpolarized agent *in vivo* could be achieved by using the singlet states of low gamma ( $\gamma$ ) nuclei.<sup>9</sup> However, as NMR receptivity scales as  $\gamma^3$  for spin  $1/2$  nuclei, direct NMR detection of low  $\gamma$  nuclei results in a lower signal-to-noise ratio compared to proton detection. While protons are better nuclei for detection, short spin lattice relaxation times prevent direct  $^1\text{H}$  hyperpolarized MR in biomedical applications.

Here, we demonstrate the utility of  $^{13}\text{C}$  for spin storage of hyperpolarization followed by  $^1\text{H}$  detection using INEPT,<sup>10</sup> which theoretically can provide up to an  $(\gamma_{\text{H}}/\gamma_{\text{X}})^2$  gain in sensitivity in hyperpolarized biomedical MR. Specifically, we hyperpolarized the  $^{13}\text{C}$  site of two well studied molecules,  $1\text{-}^{13}\text{C}$ -succinate- $d_2$ <sup>5,11</sup> and 2,2,3,3-tetrafluoropropyl  $1\text{-}^{13}\text{C}$ -propionate- $d_3$  (TFPP), by PASADENA (Figure 1). Both molecules are accessible from unsaturated precursors containing a double bond by molecular cis addition of parahydrogen. Hyperpolarized succinate<sup>5,11</sup> can be potentially exploited as a metabolic biomarker of cancer, while hyperpolarized TFPP has been shown to be a specific binder to lipids with a unique chemical shift signature in the lipid bound state<sup>12</sup> potentially useful for plaque imaging.<sup>13</sup>

Parahydrogen addition and transfer of spin order to  $^{13}\text{C}$  has been described previously.<sup>5,14</sup> A home-built PASADENA polarizer was employed to hydrogenate 2,2,3,3-tetrafluoropropyl  $1\text{-}^{13}\text{C}$ -acrylate- $d_3$  (TFPA) to yield hyperpolarized TFPP and  $1\text{-}^{13}\text{C}$ -fumarate- $d_2$  (CIL, Andover, MA) to yield hyperpolarized  $1\text{-}^{13}\text{C}$ -succinate- $d_2$  in deuterated solvent. The spin order transfer was performed using an untuned saddle coil at 1.76 mT utilizing the heteronuclear spin order transfer pulse sequence described by Goldman and Johansson<sup>15</sup> and was tailored to the hetero- and homonuclear  $J$  coupling of propionate<sup>14,16</sup> for TFPP and succinate at pH 11 (Figure 2).<sup>5</sup>

*In vitro*  $1\text{-}^{13}\text{C}$  succinate spin lattice relaxation time  $T_1$  is  $105 \pm 1$  s in  $\text{D}_2\text{O}$  at pH 11, and *in vivo*  $T_1$  is in excess of 43 s at 4.7 T, which is significantly longer than the previously published values at pH 3.<sup>5</sup> *In vitro*  $1\text{-}^{13}\text{C}$  TFPP  $T_1 = 67 \pm 1$  s in deuterated medium, and *in vivo*  $T_1$  is in excess of 16 s at 4.7 T.<sup>13</sup> Such long spin lattice relaxation times provide an efficient storage of spin polarization in long-lived low  $\gamma$  nuclear spin states, which is exemplified here by  $^{13}\text{C}$  TFPP and

succinate. The principal motivation for development of long-lived nuclear spin states is their utility to monitor biochemical pools *in vivo* such as stable isotope enrichment of metabolic events or receptor binding. NMR signal detection utilizing polarization transfer from long-lived low  $\gamma$  nuclear spin states to  $J$ -coupled protons provides a potential to further increase the MR signal in such studies (Figure 2) utilizing the strategy of two sequential polarization transfers.<sup>17</sup>

In one experiment, 2.4 mL of 6.2 mM  $1\text{-}^{13}\text{C}$ -succinate- $d_2$  were hyperpolarized at the  $^{13}\text{C}$  site to 10.7%. Hyperpolarization was then kept on  $^{13}\text{C}$  for 70 s. During this time, the polarized sample was

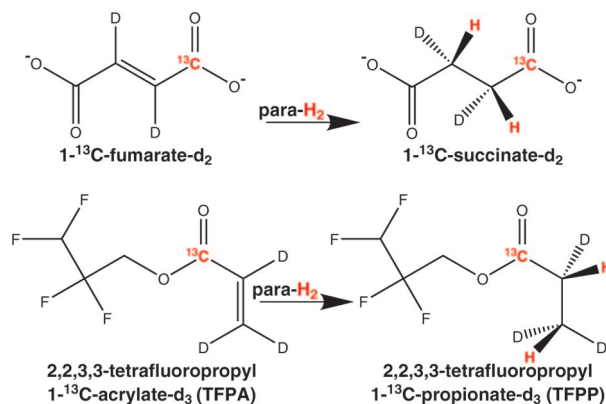


**Figure 1.** Cis molecular addition of parahydrogen to  $1\text{-}^{13}\text{C}$ -fumarate- $d_2$  to produce  $1\text{-}^{13}\text{C}$ -succinate- $d_2$  and cis molecular addition of parahydrogen to TFPA to produce TFPP. The catalytic reaction was carried out at  $60^\circ\text{C}$  in  $\text{D}_2\text{O}$  with reactant concentrations of 3–6 mM. TFPP aqueous solution used 10% v/v acetone- $d_6$  necessary to dissolve hyperpolarized product.

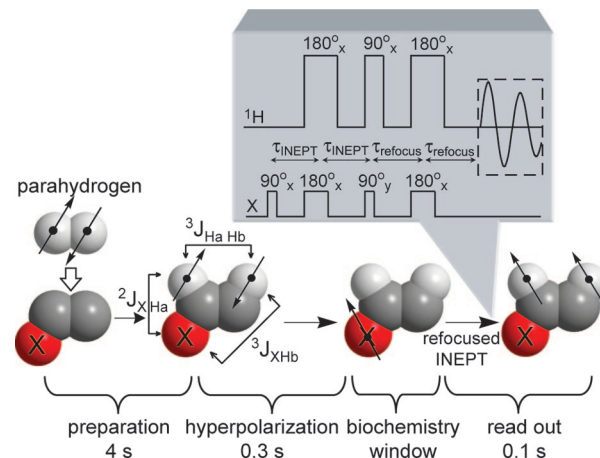


**Figure 2.** The experimental diagram of molecular cis addition of parahydrogen followed by hyperpolarization of X nucleus exemplified by  $^{13}\text{C}$ , polarization storage on X nucleus (potentially allowing monitoring of biochemical events on the time scale of minutes) followed by polarization transfer back to more sensitive protons for NMR detection.

<sup>†</sup> Huntington Medical Research Institutes.

<sup>‡</sup> California Institute of Technology.

transferred from a low magnetic field polarizer operating at 1.76 mT to a 4.7 T animal MR scanner. The  $^{13}\text{C}$  polarization decayed from 10.7% to 5.5% corresponding to the final  $^{13}\text{C}$  signal enhancement by a factor of 13 500. Then the refocused INEPT pulse sequence<sup>10</sup> with  $\tau_{\text{INEPT}} = 34$  ms and  $\tau_{\text{refocus}} = 32$  ms (Figure 2) was used to transfer polarization from  $^{13}\text{C}$  to protons within 1- $^{13}\text{C}$ -succinate- $d_2$  (Figure 3A and 3B). We found that the two protons were successfully hyperpolarized corresponding to 41% polarization transfer efficiency and 1350-fold  $^1\text{H}$  NMR signal enhancement per two methylene protons. In a separate experiment, 2.4 mL of 2.9 mM TFPP were polarized to 14%, and the hyperpolarization was stored on the 1- $^{13}\text{C}$  site for 24 s, during which the polarization decayed to 9.5% corresponding to a final signal enhancement of 23 300-fold at this site (Figure 3E). The delays of the refocused INEPT were  $\tau_{\text{INEPT}} = 20$  ms and  $\tau_{\text{refocus}} = 16$  ms. The combined intensity of the three NMR lines corresponding to four hydrogen atoms (Figure 3F) was enhanced by a factor of 2930, corresponding to the 50% polarization transfer efficiency by the refocused INEPT sequence.

To quantify the degree of hyperpolarization, we used the reference of a single scan spectrum of thermally polarized 100% natural abundance ethanol (Figure 3A) and 3 M sodium 1- $^{13}\text{C}$ -acetate (Figure 3B) at 4.7 T using the formula:

$$\%P_X = \frac{\chi_{\text{ref}}}{\chi_{\text{expt}}} \cdot \frac{S_{\text{expt}}}{S_{\text{ref}}} \cdot \frac{P_X^0}{\sin \theta} \cdot 100\%$$

where  $P_X^0$  is the nuclear polarization at equilibrium at 298 K and 4.7 T, according to the Boltzmann distribution,  $\theta$  is the angle of the detection pulse,  $\chi_{\text{ref}}$  and  $\chi_{\text{expt}}$  are the molar concentrations of sites in the reference and the experimental molecule, respectively, and  $S_{\text{ref}}$  and  $S_{\text{expt}}$  are the signal from the reference and experimental molecular sites, respectively. Under the experimental conditions,  $P_{^{13}\text{C}}^0$  is  $246\,600^{-1}$  and  $P_{^1\text{H}}^0$  is  $62\,000^{-1}$ . The achieved  $\%P_{^1\text{H}}$  was 2.2% for 1- $^{13}\text{C}$ -succinate- $d_2$  and 4.8% for TFPP. The efficiency of the polarization transfer from  $^{13}\text{C}$  to  $^1\text{H}$  reported here, 41% for 1- $^{13}\text{C}$ -succinate- $d_2$  and 50% for TFPP, is a ratio between the  $^1\text{H}$  polarization detected after the transfer and  $^{13}\text{C}$  polarization as measured by a  $12^\circ$  excitation pulse before the INEPT transfer. While the efficiency of the polarization transfer was 50% or below, hyperpolarized protons are inherently 15.8-fold more sensitive compared to hyperpolarized  $^{13}\text{C}$ . As a result, proton detection of hyperpolarized 1- $^{13}\text{C}$ -succinate- $d_2$  and TFPP increased the overall sensitivity by a factor of 6.5 and 7.9, respectively.

The method demonstrated herein can potentially be applied to these and other hyperpolarized  $^{13}\text{C}$  metabolic contrast agents *in vivo* including hyperpolarized pyruvate,<sup>18</sup> lactate, bicarbonate,<sup>6</sup> alanine, glutamine,<sup>7</sup> and choline.<sup>8</sup> More importantly, using this approach, hyperpolarized  $^{15}\text{N}$  MR would become an attractive biomedical tool due to the much longer spin lattice relaxation time owing to low  $\gamma$ , but now with the added advantage of more sensitive detection using proton NMR ( $\gamma_{^{15}\text{N}}^2 \approx \gamma_{^1\text{H}}^2/100$ ). Furthermore, proton imaging, localized spectroscopy, and chemical shift imaging (CSI) will allow improved spatial resolution by  $\gamma_{^1\text{H}}/\gamma_X$  in each dimension at a given gradient strength.

**Acknowledgment.** We thank Drs. Brian D. Ross and William H. Perman and the following for funding: NIH 1K99CA134749-01, R01 CA 122513, 1R21 CA118509, Rudi Schulte Research Institute, James G. Boswell Fellowship, AHA, American Brain Tumor Association, Beckman Institute, Tobacco Related Disease Research Program 16KT-0044, Prevent Cancer Foundation.

## References

- (1) Bowers, C. R.; Weitekamp, D. P. *Phys. Rev. Lett.* **1986**, *57*, 2645–2648.
- (2) Bowers, C. R.; Weitekamp, D. P. *J. Am. Chem. Soc.* **1987**, *109*, 5541–5542.
- (3) Abragam, A.; Goldman, M. *Rep. Prog. Phys.* **1978**, *41*, 395–467.
- (4) Golman, K.; in't Zandt, R.; Thanning, M. *Proc. Natl. Acad. Sci. U.S.A.* **2006**, *103*, 11270–11275.
- (5) Chekmenev, E. Y.; Hovener, J.; Norton, V. A.; Harris, K.; Batchelder, L. S.; Bhattacharya, P.; Ross, B. D.; Weitekamp, D. P. *J. Am. Chem. Soc.* **2008**, *130*, 4212–4213.
- (6) Gallagher, F. A.; Kettunen, M. I.; Day, S. E.; Hu, D. E.; Ardenkjaer-Larsen, J. H.; in't Zandt, R.; Jensen, P. R.; Karlsson, M.; Golman, K. *Nature* **2008**, *453*, 940–U973.
- (7) Gallagher, F. A.; Kettunen, M. I.; Day, S. E.; Lerche, M.; Brindle, K. M. *Magn. Reson. Med.* **2008**, *60*, 253–257.
- (8) Gabellieri, C.; Reynolds, S.; Lavie, A.; Payne, G. S.; Leach, M. O.; Eykyn, T. R. *J. Am. Chem. Soc.* **2008**, *130*, 4598–4599.
- (9) Pileio, G.; Carravetta, M.; Hughes, E.; Levitt, M. H. *J. Am. Chem. Soc.* **2008**, *130*, 12582–12583.
- (10) Morris, G. A.; Freeman, R. *J. Am. Chem. Soc.* **1979**, *101*, 760–762.
- (11) Bhattacharya, P.; Chekmenev, E. Y.; Perman, W. H.; Harris, K. C.; Lin, A. P.; Norton, V. A.; Tan, C. T.; Ross, B. D.; Weitekamp, D. P. *J. Magn. Reson.* **2007**, *186*, 150–155.
- (12) Chekmenev, E. Y.; Chow, S. K.; Tofan, D.; Weitekamp, D. P.; Ross, B. D.; Bhattacharya, P. *J. Phys. Chem. B* **2008**, *112*, 6285–6287.
- (13) Chekmenev, E. Y.; et al. *Angew. Chem., Int. Ed.*, submitted.
- (14) Bhattacharya, P.; Harris, K.; Lin, A. P.; Mansson, M.; Norton, V. A.; Perman, W. H.; Weitekamp, D. P.; Ross, B. D. *Magn. Reson. Mat. Phys. Biol. Med.* **2005**, *18*, 245–256.
- (15) Goldman, M.; Johannesson, H. C. R. *Physique* **2005**, *6*, 575–581.
- (16) Goldman, M.; Johannesson, H.; Axelsson, O.; Karlsson, M. C. R. *Chimie* **2006**, *9*, 357–363.
- (17) Aime, S.; Gobetto, R.; Reineri, F.; Canet, D. *J. Chem. Phys.* **2003**, *119*, 8890–8896.
- (18) Golman, K.; in't Zandt, R.; Lerche, M.; Pehrson, R.; Ardenkjaer-Larsen, J. H. *Chem. Res.* **2006**, *66*, 10855–10860.

JA809634U

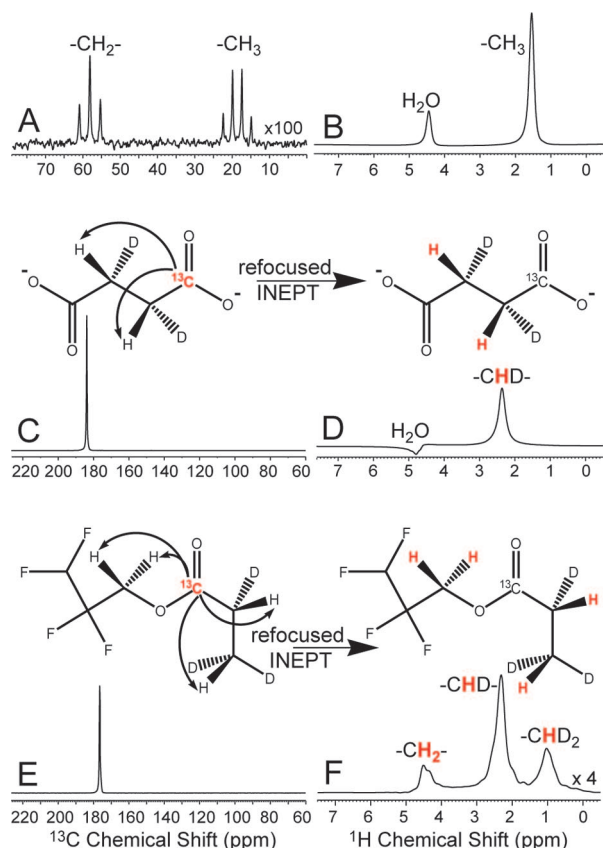


**Figure 3.** (A)  $^{13}\text{C}$  reference spectrum of 2.8 mL of 17 M ethanol with 188 mM  $^{13}\text{C}$  concentration per site. (B)  $^1\text{H}$  NMR spectrum of 2.8 mL of 3 M sodium  $^{13}\text{C}$ -acetate in  $\text{D}_2\text{O}$ . (C)  $^{13}\text{C}$  NMR spectrum of hyperpolarized 6.2 mM 1- $^{13}\text{C}$ -succinate- $d_{2,3}$ ,  $^{13}\text{C}$  polarization of 5.5% after being stored for 70 s,  $T_1 = 105$  s, the spectrum is acquired using a  $12^\circ$  excitation pulse. (D)  $^1\text{H}$  NMR spectrum of hyperpolarized 6.2 mM 1- $^{13}\text{C}$ -succinate- $d_{2,3}$  where net  $^1\text{H}$  signal enhancement is 1350-fold with 41% spin polarization transfer efficiency. (E)  $^{13}\text{C}$  NMR spectrum of hyperpolarized 2.9 mM TFPP.  $^{13}\text{C}$  polarization is 9.5% after being stored for 24 s,  $T_1 = 67$  s. The spectrum is acquired using a  $12^\circ$  excitation pulse. (F)  $^1\text{H}$  NMR spectrum of hyperpolarized 2.9 mM TFPP where net  $^1\text{H}$  signal enhancement is 2930-fold with 51% efficiency.